

Boiling Heat Transfer in Copper Foam Bilayers in Positive and Inverse Gradients of Pore Density

H. Wang^{1,2†}, Q. F. Ying¹, E. Lichtfouse³ and C. G. Huang¹

¹ College of Environmental Science and Engineering, Donghua University, Shanghai, 201620, China

² State Key Laboratory for Modification of Chemical Fibers and Polymer Materials, Donghua University, Shanghai, 201620, China

³ Aix Marseille Univ, CNRS, IRD, INRAE, CEREGE, Aix-en-Provence, 13007, France

†Corresponding Author Email: huiwang@dhu.edu.cn

(Received October 24, 2022; accepted January 24, 2023)

ABSTRACT

Gradient metal foam is an advanced heat transfer material that decreases resistance to bubble escape and enhances the transfer of boiling heat. In this study, boiling heat transfer and bubble behavior were studied in an experimental set-up with copper foam bilayers configured either in positive or inverse gradients, utilizing deionized water as working fluid. Positive gradient refers to arranging metal foam layers with high pore density at the bottom, above the heat source, and low pore density on the top. Results show that the heat transfer is higher for gradient metal foam surfaces, of 6.14×10^5 W/m², versus a uniform metal foam surface, of 3.94×10^5 W/m². For the positive gradient configuration, boiling heat transfer performance first increased with the pore density, then decreased when the pore density was higher than 60 pores per inch (PPI). By contrast, for the inverse gradient, the heat transfer performance was nearly constant with increasing pore density. At the low pore density, the inverse gradient performed better than the positive gradient during the whole boiling process. At high pore density, the positive gradient structure performed better in heat transfer at the early boiling stage. Three main types of bubble escape were observed: For the positive gradient bilayer, the bubbles moved up or down without lateral interference. In contrast, for inverse gradient, the bubbles mostly escape from the sides, which is easy to induce bubble merging. The inverse gradient surface generates larger bubbles, while the positive gradient surface produces a higher frequency of bubble detachment. Accordingly, two liquid replenishment models are proposed: for the positive gradient, external liquid replenishes from the side into the copper foam, while for inverse gradient, the liquid is mainly replenished from the top.

Keywords: Gradient copper foam; Liquid replenishment; Bubble behavior; Heat transfer enhancement; Multiphase flow.

NOMENCLATURE

d	metal foam pore size	ΔT	wall superheat
h	surface coefficient of heat transfer	V	volume of metal foam per layer
H	thickness	x	distance from the thermocouple to block bottom (m)
n	layer numbers	λ	thermal conductivity
PPI	pores per inch	ω	pore density
q	heat flux	ε	porosity
S	total heat transfer area	$\Delta\omega$	pore density difference

1. INTRODUCTION

Since electronic devices are getting smaller and more complex on the microscale, high local temperatures are threatening the stability and performance of the devices. As a consequence, the efficient thermal control of electronic components

has become a research hotspot. (He *et al.* 2021). For instance, boiling heat transfer is favored because it is possible to attain high heat flux without high superheating. Traditional ways to enhance boiling heat transfer include adjusting the operating pressure and temperature difference (Fan *et al.* 2021), roughening the heating surface (Kurihara and Myers 1960; Armin *et al.* 2021; Robert and

Robert 2021), increasing heat transfer area (Zhang *et al.* 2021), changing the surface wettability using a new type of work-piece (Zhu *et al.* 2010; Zhao *et al.* 2017; Moha and Ference 2020; Hyungdae and Eok 2021; Zhou *et al.* 2022), and making a porous metal surface (Jun *et al.* 2016; Gupta and Misra 2019; Katarkar *et al.* 2021). In particular, metal foam is an advanced porous media, with the advantages of high porosity, high thermal conductivity, and large specific surface area (Wang *et al.* 2020). Metal foams can effectively expand the heat transfer contact area and increase the bubble nucleation points for boiling heat transfer, so as to enhancing boiling heat transfer, by comparison with smooth metal surfaces (Wang and Guo 2016; Yang *et al.* 2022).

The pool boiling heat transfer of metal foam surfaces has been recently investigated. For example, Manetti *et al.* (2020) found that metal foam surfaces have advantages for liquid absorption and diffusion, thereby augmenting boiling heat transfer. Moghaddam *et al.* (2003) experimentally found that copper foam of 30 pores per inch (PPI) enhances the boiling heat exchange, whereas copper foam of 80 PPI shows no effect. Similarly, in the pool boiling experiment with acetone as the working fluid, Xu *et al.* (2008) found that copper foam with lower pore density has better heat transfer in the low heat flux region, and high pore density copper foam has better heat transfer in the medium to high heat flux region. Jia *et al.* (2017) observed that copper foam of 10-20 PPI enhanced heat transfer during the initial boiling stage. Copper foam with a higher number of pores is more conducive to enhanced the boiling heat transfer, yet this enhancement weakened when the PPI reached 50. Liu *et al.* (2021) even found that high pore density copper foam decreases boiling heat transfer. This issue may be solved by the use of gradient metal foam.

Gradient metal foam is usually formed by welding multiple layers of cell modules with different structural parameters. The gradient structure should provide an easier path for escaping bubbles, compared to metal foam of uniform pore density (Xu *et al.* 2015a). This was confirmed by the

wettability study of An *et al.* (2021) who observed that heat transfer is increased with a bilayer of copper and nickel foams, versus single layers. Studying structural parameters and arrangement order of nickel-copper double layer metal foams, Xu *et al.* (2015b), and Xu and Qin (2018) found that heat transfer is highly controlled by the layer order. Zhang *et al.* (2018) observed that the nature of the fluid also controlled heat transfer in gradient metal foams, e.g. sodium dodecyl sulfate improves, whereas *n*-heptanol declines heat transfer.

Mo *et al.* (2020) experimentally found that metal foams with radial pore density gradient produced bubbles at a higher rate during pool boiling, resulting in more intense heat transfer, compared with metal foams with uniform pore density. Ma *et al.* (2021) reported a similar observation and suggested that the radial pore density gradient could be adjusted for bubble separation and liquid replenishment to achieve higher boiling heat transfer rate. Zhou *et al.* (2018) studied bubble departure under different layers of metal foam, and found that bubble departure weakened with the increase of layers. Three modes for the separation of boiling bubbles have been proposed (Mao *et al.* 2015, Huang *et al.* 2018).

Overall, while gradients of metal foam layers are clearly more efficient than a single metal foam layer for heat transfer, the mechanisms and effects using gradients are unclear. For instance, there are few studies on the effect of the arrangement order of metal foam layers on heat transfer and bubble escape. Here we studied heat transfer and bubble escape in a monolayer of copper foam, as control, and bilayers of copper foam of different pore size arranged in positive or inverse gradients, using deionized water as working fluid.

2. EXPERIMENTAL SETUP AND PROCEDURES

2.1 Experimental Setup

Figure 1 shows the system for monitoring the boiling heat exchange.

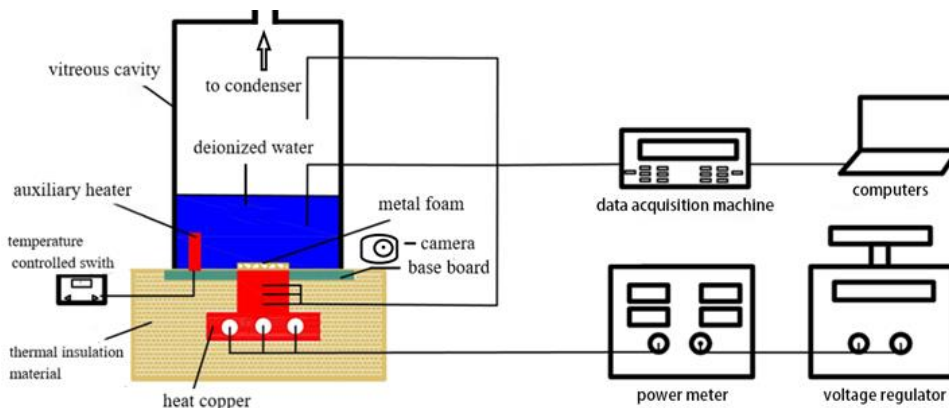


Fig. 1. Experimental setup to study the heat transfer in metal foam layers. The camera is used to observe bubble escape from the metal foam.

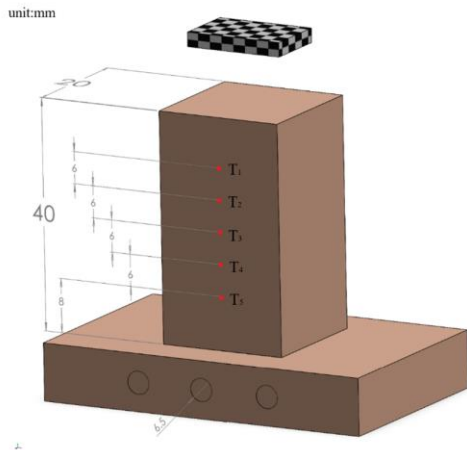


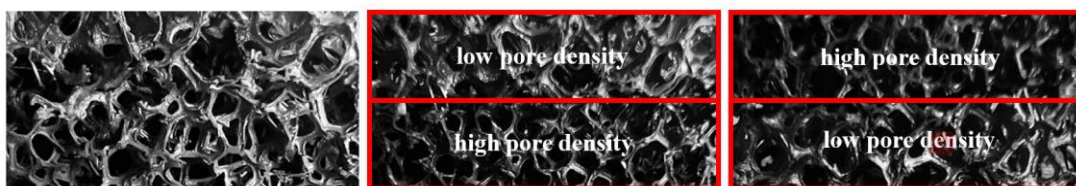
Fig. 2. Thermocouple arrangement diagram.

The heat supply system is made up of a heating copper block, an auxiliary heater, a regulator and a power meter. The size of the glass chamber ($L \times W \times H$) is 100 mm \times 100 mm \times 250 mm. The outer wall of the chamber was covered with four pieces of 10 mm thick plexiglass to reduce heat loss.

The bottom plate is made of teflon, and in its center, there is a small square hole with a side length of 21 mm, enabling the copper block to be placed exactly inside the square hole and the working fluid to be in direct contact with the copper surface. Six thermocouples are arranged to measure temperature. The thermocouple arrangement was shown in Fig. 2, the measuring point T_1 is 8 mm away from the copper surface, and then one monitoring point is arranged every 6 mm, a total of five monitoring points, namely T_1 - T_5 . T_6 is placed in a vitreous cavity to measure the temperature of the working fluid.

2.2 Materials and Procedures

Figure 3 shows the three copper foam structures. Figure 3a displays a metal foam monolayer of uniform pore density, as control. Figure 3b depicts a positive gradient made of a bilayer of copper foam, in which the high pore density is at the bottom, near the heating surface, and the low pore density is at the top. Figure 3c shows the inverse gradient metal foam, with a reversed arrangement, that is the low pore density is at the bottom and the high pore density is on the top. The pore density of the metal



(a) Uniform

(b) Positive gradient

(c) Inverse gradient

Fig. 3. Arrangements of metal foam layers.

foam varies from 10 PPI to 90 PPI, the porosity is fixed at 0.96. The length and width of each layer are both 20 mm. The total thickness of the gradient metal foam is 10 mm, which consists of two pieces of 5 mm copper foam.

Before the pool boiling experiment, the heated copper block needs to be polished with sandpaper to make its surface as smooth as possible, so as to reduce the existence of gasification core and increase the accuracy of the experiment. The surface of the copper block is then cleaned with methanol, followed by welding. The solder is rolled to obtain a layer of approximately 0.1 mm thickness and placed on top of the copper block, and then the regulator is turned on to heat it so that the solder covers the entire top surface of the copper block. When the solder is fully melted, the heat is stopped and the metal foam is quickly placed on top of the heated copper block. At the same time, heavy weights are pressed on the metal foam to ensure a tight connection (Fig. 4). The thickness of the solder layer, of 0.1mm, which is not the same order of magnitude as the size of metal foam. Therefore, its thermal resistance is usually ignored in previous studies. The experimental procedure is detailed in our previous study (Huang *et al.* 2023).



Fig. 4. Metal foam soldered to a heated copper block.

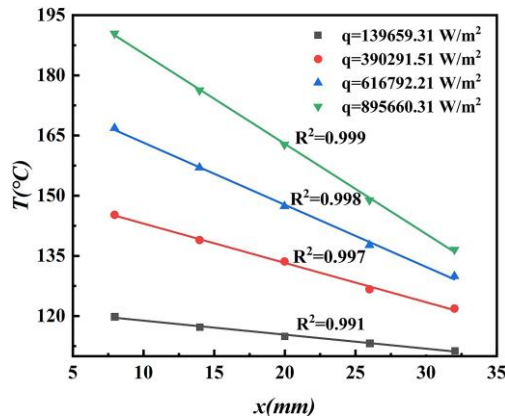


Fig. 5. Verification of one-dimensional heat conduction under different heat flux.

2.3 Experimental and Calculation Uncertainty Analysis

Figure 5 shows the change of temperature inside the heated copper block under four different heat flux. The four fitted straight lines are in good agreement with the experimental data, the correlation coefficient R^2 are all higher than 0.99. This demonstrates that the heat transfer inside the heated copper block is a one-dimensional heat conduction in the vertical direction.

The heat flux q can be calculated using the following correlation:

$$q = -\lambda \left. \frac{dT}{dx} \right|_x = -\lambda \left(\frac{T_5 - T_4}{L} + \frac{T_5 - T_3}{2L} + \frac{T_5 - T_2}{3L} + \frac{T_5 - T_1}{4L} \right) / 4 \quad (1)$$

Where λ is the thermal conductivity of the copper block, L is the distance between two adjacent thermocouples.

Superheat degree ΔT calculation formula is as follows:

$$\Delta T = T_w - T_s \quad (2)$$

Where T_w is the temperature at the top of the heating copper block, T_s is the temperature of the saturation temperature of the water.

According to the Newton cooling formula:

$$h = q / \Delta T = q / (T_w - T_s) \quad (3)$$

According to the uniform metal foam model (Du *et al.* 2012), the total surface area of heat transfer of copper foam can be expressed as follows:

$$S_{total} \approx \sum_{i=1}^n V_i \sqrt{4(\pi + \pi^2)(1 - \epsilon_i)} / d_{pi} \quad (4)$$

Where n is the layer value of gradient metal foams, V is the volume occupied by each layer of metal foam and d_p is metal foam pore size. The calculation formula is as follows:

$$V = 0.02 \times 0.02 \times H \quad (5)$$

$$d_p = 0.0254 / \omega \quad (6)$$

Where H is the metal foam thickness and ω is metal foam pore density.

Substituting Eq. (5) (6) into Eq. (4) to get S_{total} of the gradient metal foams.

$$S_{total} \approx \sum_{i=1}^n 0.02 \times 0.02 \times H_i \times \omega_i \times \sqrt{4(\pi + \pi^2)(1 - \epsilon_i)} / 0.0254 \dots \dots \dots (7)$$

The main error source of the heat flux and heat transfer coefficient came from the location of the monitoring point and its measurement method. The two relative errors are calculated in Eq. (8) and (9) (Moffat 1988, Sarangi *et al.* 2015):

$$\frac{\Delta q}{q} = \sqrt{\left(\frac{\Delta T}{T}\right)^2 + \left(\frac{\Delta L}{L}\right)^2 + \left(\frac{\Delta \lambda}{\lambda}\right)^2} \leq \frac{\Delta T}{T} + \frac{\Delta L}{L} + \frac{\Delta \lambda}{\lambda} \quad (8)$$

$$\frac{\Delta h}{h} = \sqrt{\left(\frac{\Delta T_w}{T_w - T_s}\right)^2 + \left(\frac{\Delta q}{q}\right)^2 + \left(\frac{\Delta T_s}{T_w - T_s}\right)^2} \leq \frac{\Delta T_w}{T_w - T_s} + \frac{\Delta q}{q} + \frac{\Delta T_s}{T_w - T_s} \quad (9)$$

After analysis, the error caused by calculation of q and T_w is less than 10%, which is reasonable. The temperature measurement of the thermocouple can be considered accurate, with an error of only 0.5% and within 1 K of the actual value. The error of λ and L is 3.1% and 3.3% respectively. 6.9% is the maximum uncertainty of heat flux.

3. RESULTS AND DISCUSSION

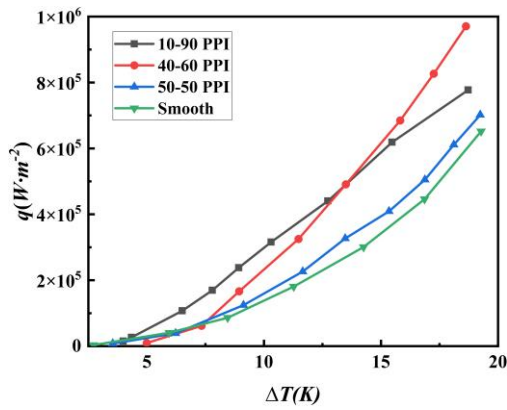
3.1 Effect of Gradient Difference

We designed three bilayers of copper foams of different pore density, 10 (top)-90 (bottom), 40-60 and 50-50 PPI, of 80, 20 and 0 PPI of gradient difference, respectively (Eq. 7, Table 1), to study their heat transfer.

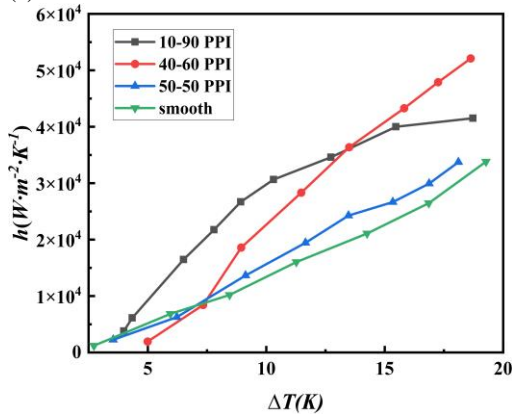
Results show that all copper foam surfaces display higher heat flux and heat transfer than the smooth copper surface used as control (Fig. 6). For example, when the superheat degree is 15 K, the

Table 1 Metal foam structure parameters.

Number	Material	ω (PPI)	H (mm)	ϵ	S_{total} (m ²)
1	Copper foam	10-90	5-5	96%	0.011360957
2		40-60	5-5	96%	0.011360957
3		50-50	5-5	96%	0.011360957



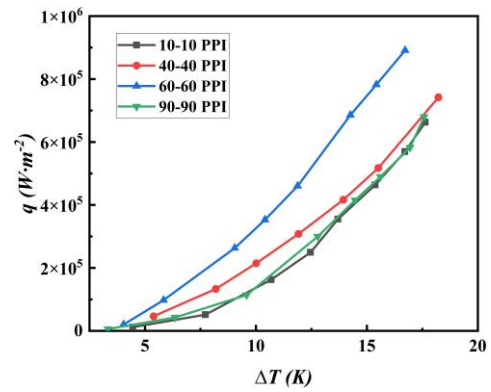
(a) Heat flux



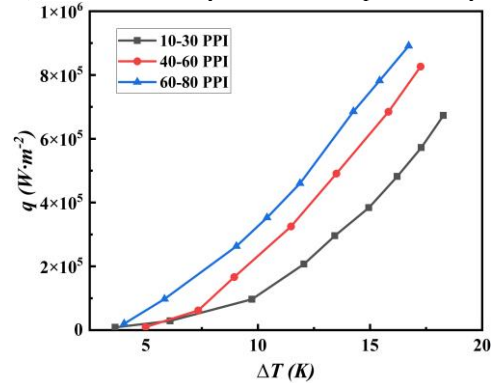
(b) Heat transfer coefficient

Fig. 6. Effect of different gradient differences on pool boiling heat transfer for the same heat transfer area. Gradient layers are arranged positively from the top layer toward the bottom layer, e.g. 10-90 refers to a two layer composite with a top layer of 10 PPI pore density and a bottom layer of 90 PPI pore density.

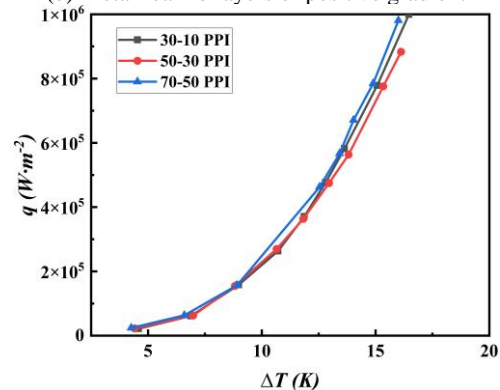
heat flux for smooth surface is $2.68 \times 10^5 \text{ W/m}^2$, while they are 3.94×10^5 , 5.88×10^5 and $6.14 \times 10^5 \text{ W/m}^2$ for 50-50, 10-90 and 40-60 PPI. In the initial boiling period, when the superheat is low and fewer bubbles escape, The replenishment rate of liquid is the main factor that determines the heat transfer of boiling. The metal foam bilayer with a step difference of 80 PPI (10-90 PPI) has the largest pore in the top layer of 10 PPI, which is conducive to liquid replenishment, so it shows higher performance. During boiling, however, the superheat increases and more bubbles escape. The number of nucleation points and bubble escape rate become the main factors controlling heat transfer. The bilayer with a step difference of 20 PPI (40-60 PPI) becomes the most effective. This is because the upper layer has a higher pore density of 40 PPI, and the total heat transfer area and bubble nucleation point are also higher, which is conducive to the development of pool boiling heat transfer. However, it was noted that although 50-50 PPI had a higher pore density, the performance was poor because the high pore density prevented the bubble from escaping and was not conducive to heat transfer.



(a) Metal foam bilayers of uniform pore density



(b) Metal foam bilayers of positive gradient



(c) Metal foam bilayers of inverse gradient

Fig. 7. Effect of pore density on boiling heat transfer performance under three gradient metal foam. Gradient layers are arranged from the top layer toward the bottom layer, e.g. 10-30 refers to a two layer composite with a top layer of 10 PPI pore density and a bottom layer of 30 PPI pore density.

3.2 Effect of Pore Density

Figure 7 shows the effect of pore density on boiling heat transfer under three gradient metal foam. As shown in Fig. 7a, The results show that for uniform gradient, when the pore density is less than 60 PPI, the increase of pore density leads to the increase of bubble nucleation point and heat transfer surface area. Therefore, the boiling heat transfer performance of uniform metal foam is directly proportional to the pore density. Whereas, when the pore density exceeds 60 PPI, the effect of metal foam on enhancing the boiling process is greatly

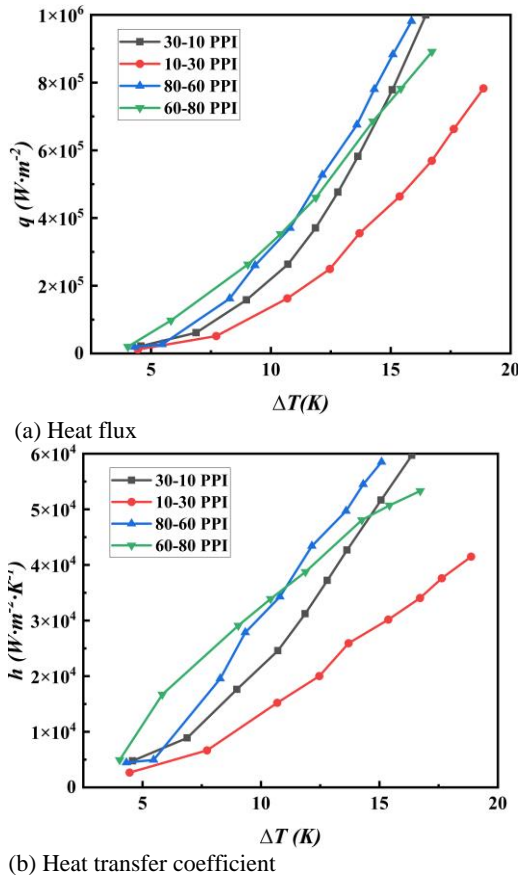


Fig. 8. Heat transfer performance of positive and inverse gradient bilayers of metal foam
a) heat flux, b) heat transfer coefficient.

weakened due to the increase of bubble escape resistance. The 60-60 PPI uniform bilayer has certain advantages in the number of nucleation points, heat transfer area and bubble escape ability, so the performance is better.

While for bilayer positive gradient, as shown in Fig. 7b), the boiling heat transfer performance does not decrease with the increase of pore density. The 60-80 PPI bilayer depicting the highest performance, because the pore size of the upper layer is larger, the resistance of bubble escape is reduced, it is difficult to cause bubble blockage, and the liquid replenishment rate can be increased.

It is noted in Fig. 7c that the heat transfer performance of the inverse gradient bilayers of metal foam does not change significantly with the pore density, which indicates the number of bubble nucleation points and the heat transfer area are not influencing the heat transfer.

3.3 Comparison of Positive and Inverse Gradients

We compared the heat transfer performance of positive bilayer gradients, 10-30 PPI and 60-80 PPI, with their inverse counterparts, 30-10 PPI and 80-60 PPI, in Fig. 8. Results show that at low pore density the heat transfer of the inverse gradient 30-10 PPI is better than that of the positive gradient 10-30 PPI. For higher pore density of 60-80 PPI and 80-60 PPI, the positive gradient 60-80 PPI shows better heat transfer performance at the beginning of boiling. However, as the superheat increases, the boiling heat transfer with an inverse gradient of 80-60 PPI grows rapidly and exceeds the positive gradient performance at the middle and late stages of boiling.

3.4 Bubble Dynamics

Figure 9 shows the bubble dynamic behavior of metal foam with positive gradient and inverse gradient under different heat fluxes. Photos show that bubble escape is very different for positive versus inverse gradient of metal foam bilayers. Specifically, for the positive gradient, boiling bubbles are escaping vertically upward and downward. The corresponding force analysis and detachment form are explained in Fig. 10a. When the heat flux is low, the heat flow driving force F_b is small, and the bubbles cannot timely displace the surrounding liquid, resulting in the expansion of the bubble volume and escape mainly by buoyancy F_i . When the heat flux is high, both the bubble growth force F_a and the heat flow driving force F_b increase. Moreover, due to the larger pores in the upper metal foam, the bubble escape resistance F_σ is greater, which is conducive to the bubble escaping from the surface of the copper foam, which is also confirmed in Fig. 11b. Metal foam with a positive gradient (40-60 PPI) has a higher bubble departure frequency. Figure 11a shows that the bubble

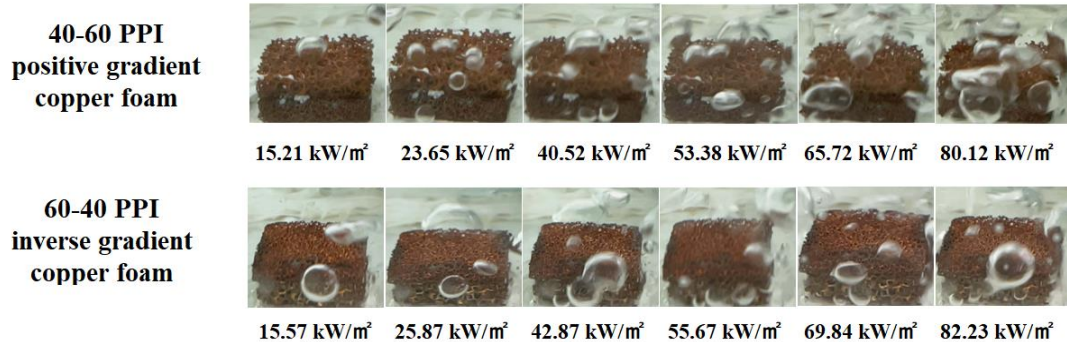


Fig. 9. Bubble dynamics versus heat flux in different arrangements of multilayers gradient copper foam.

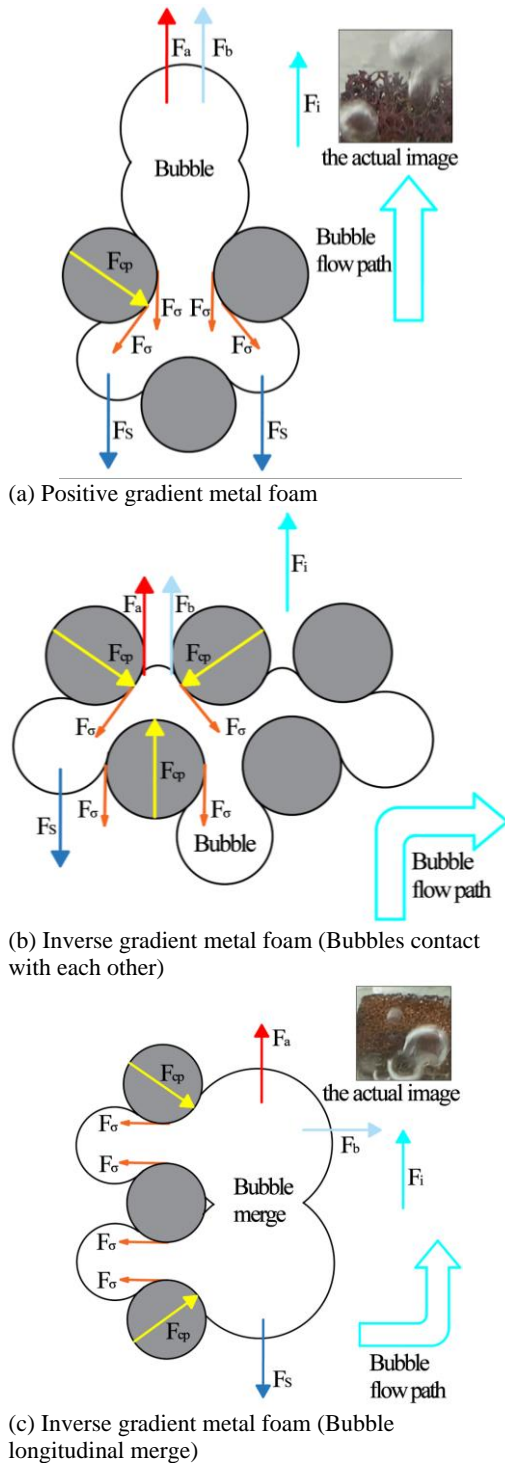


Fig.10. Positive and inverse gradients metal foam bubble detachment form, F_a is the bubble growth force, F_b is the heat flow driving force, F_i is the buoyancy force, F_{cp} is the contact pressure of the copper foam skeleton, F_s is the surface tension, and F_σ is the bubble brought by the metal foam skeleton escape resistance.

diameter increases from about 5 to 7 mm with heat flux, then decrease to a plateau at about 6 mm, probably as a result of small bubbles still produced at high heat flux, resulting in an overall

insignificant change in bubble size. At this time, the main factors that determine the boiling heat transfer performance of positive gradient metal foam are the number of bubble nucleation points and the total heat transfer area. Figure 8 illustrates this point. The metal foam with a structure of 60-80 PPI has smaller pores than that with a structure of 10-30 PPI, so it has more nucleation points and heat transfer area, and better heat transfer performance.

However, for the inverse gradient, most bubbles detach from the layer sides due to the small pore size of the upper layer (Fig. 10a). Only few small bubbles detach from the top at the late boiling stage (Fig. 10b). Here, bubbles forming inside the bottom layers cannot easily escape upward, as is demonstrated in Fig. 11b, and the inverse gradient structure (60-40 PPI) has a smaller bubble departure frequency. As a consequence, they merge together and the increasing gaseous pressure pushes bubbles horizontally to escape sideward. Once bubble escape the layers, they move upward due to buoyancy. Multiple bubbles tend to aggregate into one large bubble during escape, leading to re-absorption into the copper foam. Figure 11a shows that the bubble diameter appears to increase from about 6 to 8 mm, but these trends require further studies to be confirmed due the large fluctuations observed.

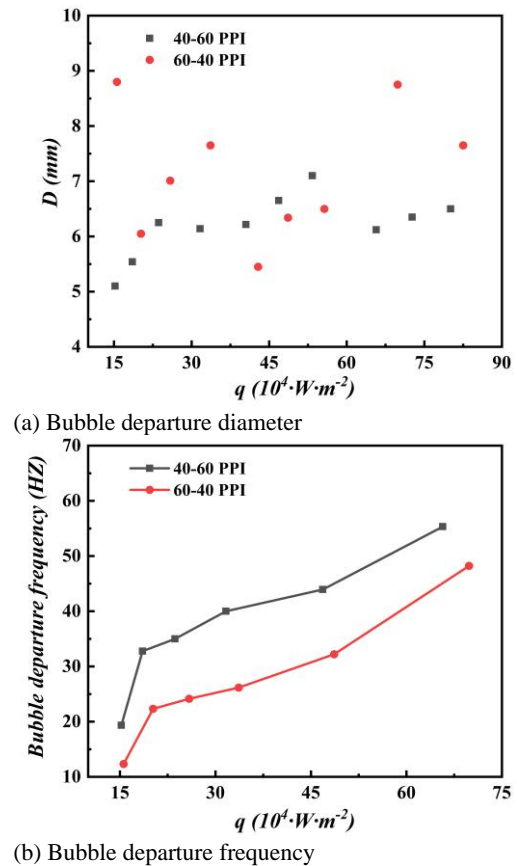


Fig. 11. Variation of the bubble departure diameter and bubble departure frequency in positive gradient and inverse gradient metal foams.

The main factor that determines the boiling heat transfer performance of inverse gradient metal foams is the liquid replenishment rate. This is confirmed in Fig. 8, when a large number of bubbles escape, the metal foam with a structure of 80-60 PPI has more liquid filling positions, but due to the high pore density, the bubble escape resistance increases, so the heat transfer performance is only slightly increased compared with the metal foam with 30-10 PPI.

3.5 Liquid Replenishment Model

The pool boiling process includes nucleation, bubble growth, bubble separation, rewetting and re-nucleation. The replenishment of external liquid is the premise for rewetting and re-nucleation of bubble nucleation, and is also an important factor affecting the heat transfer performance of pool boiling. Therefore, the amount and location of external liquid replenishment can directly affect the boiling heat transfer performance.

Figure 12 shows the liquid replenishment model under positive and inverse gradients. According to the analysis of the bubble detachment form in the previous section, when the gradient is positive, as shown in Fig.10a), the bubbles mainly detached from the top. As a consequence, it is difficult for the external liquid to replenish from the top into the copper foam layer; therefore, the liquid enters the copper foam the side (hollow blue arrow in Fig. 12a).

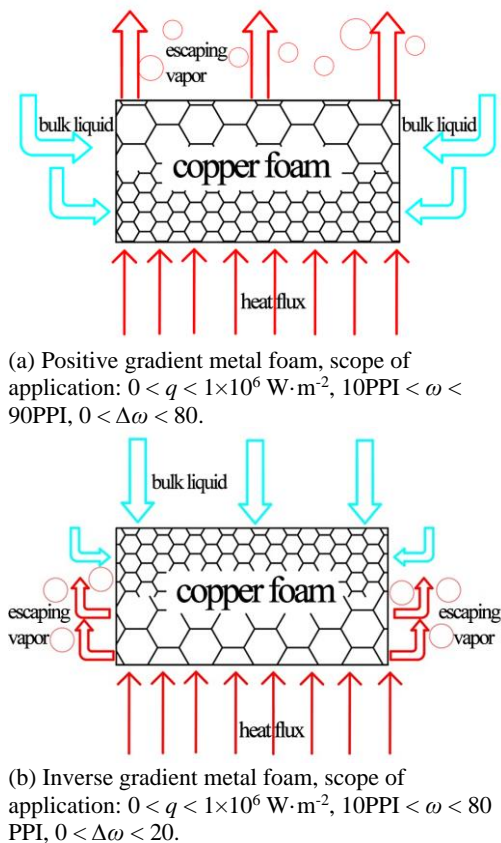


Fig. 12. Liquid replenishment model.

On the contrary, the inverse gradient structure is difficult for boiling bubbles to escape from the top because the upper pores are smaller. As shown in Fig. 10b) and Fig. 10c), most bubbles detach from the copper foam side. As a result, the liquid is mostly replenished from the top, with a small amount entering from the side (blue hollow arrow in Fig. 12b). This greatly shortens the escape path. This implies that the inverse gradient bilayer has a faster replenishing rate, which is conducive to the enhancement of boiling heat transfer.

4. CONCLUSION

In this paper, the effect of copper foam with different gradient structures on boiling heat transfer performance was investigated by visualization experiments. The effect of pore density and gradient arrangement and the bubble escape forms and liquid replenishment models are discussed for positive gradient and inverse gradient metal foams. The following conclusions are drawn:

- (1) At the early stage of boiling, copper foam bilayers of larger gradient difference show a stronger boiling heat transfer performance. At middle and late boiling stages, bilayers of lower gradient difference display the best heat transfer performance. The boiling heat transfer performance of positive gradient increases with pore density, whereas boiling heat transfer performance of the inverse gradient is almost unaffected by pore density.
- (2) When the pore density is low, the boiling heat transfer performance of the inverse gradient bilayer is stronger than the positive gradient counterpart during the whole boiling process. Whereas, when the pore density is high, the positive gradient bilayer shows better heat transfer performance at the early boiling stage.
- (3) The bubble escape forms in positive and inverse gradients are quite different, and three different bubble detachment forms are observed. For the positive gradient bilayer, the bubbles move vertically up- and downward, without lateral interference. By contrast, for the inverse gradient, the bubbles mainly escape sideward, and the bubble longitudinal merging is common. The inverse gradient surface displays larger bubbles on average, while the positive gradient surface shows higher bubble detachment frequency.
- (4) Liquid replenishment models for positive gradient and inverse gradient were constructed. For positive gradients, external liquid replenishes from the side into the copper foam. For inverse gradient, the liquid is mainly replenished from the top.

ACKNOWLEDGEMENTS

The study was funded by State Key Laboratory for Modification of Chemical Fibers and Polymer Materials, Donghua University(KF2123).

REFERENCES

- An, Y., C. Huang and X. Wang (2021). Effects of thermal conductivity and wettability of porous materials on the boiling heat transfer. *International Journal of Thermal Sciences* 170, 107110.
- Armin, S., T. Outi and C. Mauro (2021). Effects of surface nanostructure and wettability on pool boiling: A molecular dynamics study. *International Journal of Thermal Sciences* 167, 106980.
- Du, Y. P., C. Y. Zhao and Y. Tian (2012). Analytical considerations of flux boiling heat transfer in metal-foam filled tubes. *Heat and Mass Transfer* 48(1), 165-173.
- Fan, X. G., L. Yang and M. Zhang (2021). Saturated pool boiling with HFE-7100 on a smooth copper surface under different pressures. *Chemical Industry and Engineering Progress* 40(01), 57-66.
- Gupta, S. K. and R. D. Misra (2019). An experimental investigation on pool boiling heat transfer enhancement using Cu-Al₂O₃ nanocomposite coating. *Experimental Heat Transfer* 32(2), 133-158.
- He, Z., Y. Yan and Z. Zhang (2021). Thermal management and temperature uniformity enhancement of electronic devices by micro heat sinks: A review. *Energy* 216, 119223.
- Huang, C. G., H. Wang and E. Lichtfouse (2023). Experimental study of multilayer gradient copper foam effect on pool boiling heat transfer performance and gas-liquid behavior characteristics. *International Journal of Thermal Sciences* 183, 107856.
- Huang, R. L., C. Y. Zhao and Z. G. Xu (2018). Investigation of bubble behavior in gradient porous media under pool boiling conditions. *International Journal of Multiphase Flux* 103, 85-93.
- Hyungdae, K. and K. D. Eok (2021). Effects of surface wettability on pool boiling process: Dynamic and thermal behaviors of dry spots and relevant critical heat flux triggering mechanism. *International Journal of Heat and Mass Transfer* 180, 121762.
- Jia, X., J. Shi and Z. Chen (2017). Single bubble rising dynamics in porous media using lattice Boltzmann method. In *IOP Conference Series: Earth and Environmental Science*, IOP Publishing.
- Jun, S., J. Kim and D. Son (2016). Enhancement of pool boiling heat transfer in water using sintered copper microporous coatings. *Nuclear Engineering and Technology* 48(4), 932-940.
- Katarkar, A. S., A. D. Pingale and S. U. Belgamwar (2021). Experimental study of pool boiling enhancement using a two-step electrodeposited Cu-GNPs nanocomposite porous surface with R-134a. *Journal of Heat Transfer* 12, 121601.
- Kurihara, H. M. and J. E. Myers (1960). The effects of superheat and surface roughness on boiling coefficients. *Aiche Journal* 6(1), 83-91.
- Liu, R., Z. C. Teng and S. G. Yao (2021). Effects of different concentrations of Al₂O₃ nanoparticles and base fluid types on pool boiling heat transfer in copper foam with bottom condensed reflux. *International Journal of Thermal Sciences* 163, 106833.
- Ma, Y., C. Huang and X. Wang (2021). Experimental investigation on boiling heat transfer enhanced by gradient aperture porous copper. *Applied Thermal Engineering* 191, 116877.
- Manetti, L. L., G. Ribatski and R. Souza (2020). Pool boiling heat transfer of HFE-7100 on metal foams. *Experimental Thermal and Fluid Science* 113, 110025.
- Mao, Y. B., W. Chen and J. Wang (2015). The heat transfer characteristics of open-cell metal foams in pool boiling. *Cryogenics and Superconductivity* 43(06), 79-83.
- Mo, D. C., S. Yang and J. L. Luo (2020). Enhanced pool boiling performance of a porous honeycomb copper surface with radial diameter gradient. *International Journal of Heat and Mass Transfer* 157, 119867.
- Moffat, R. J. (1988). Describing the uncertainties in experimental results. *Experimental Thermal and Fluid Science* 1(1), 3-17.
- Moghaddam, S., M. Ohadi and J. Qi (2003). Pool boiling of water and fc-72 on copper and graphite foams. In *Asme International Electronic Packaging Technical Conference & Exhibition*.
- Moha, M. S. K. and L. Ference (2020). Enhancement of pool boiling heat transfer performance using dilute cerium oxide/water nanofluid: An experimental investigation. *International Communications in Heat and Mass Transfer* 114, 104587.
- Robert, K. P. and P. Robert (2021). Pool boiling of water on surfaces with open microchannels. *Energies* 14(11), 3062-3062.
- Sarang, S., J. A. Weibel and S. V. Garimella (2015). Effect of particle size on surface-coating enhancement of pool boiling heat transfer. *International Journal of Heat and Mass Transfer* 81, 103-113.
- Wang, H. and L. J. Guo (2016). Experimental investigation on pressure drop and heat transfer in metal foam filled tubes under convective boundary condition. *Chemical Engineering Science* 63(05), 438-448.
- Wang, H., L. J. Guo and K. Chen (2020). Theoretical and experimental advances on heat transfer and flow characteristics of metal

- foams. *Science China Technological Sciences* 155, 705-718.
- Xu, J. L., X. B. Ji and W. Zhang (2008). Pool boiling heat transfer of ultra-light copper foam with open cells. *International Journal of Multiphase Flow* 34(11), 1008-1022.
- Xu, Z. G. and J. Qin (2018). Pool boiling investigation on gradient metal foams with double layers. *Applied Thermal Engineering* 131, 595-606.
- Xu, Z. G., C. Y. Zhao and Y. Zhao (2015a). Experimental investigation on pool boiling heat transfer of gradient metal foams. *Journal of Engineering Thermophysics* 36(10), 2240-2244.
- Xu, Z. G., M. Q. Wang and C. Y. Zhao (2015b). Investigation on pool boiling heat transfer of metal foam with gradient pore densities. *Journal of Thermal Science and Technology* 14(02), 106-113.
- Xu, Z. G., S. Mou and Q. Wang (2018). Experimental investigation on pool boiling mechanism of two-level gradient metal foams in deionized water, aqueous surfactant solutions and polymeric additive solutions. *Experimental Thermal and Fluid Science* 96, 20-32.
- Yang, G., R. Xu and Y. Wang (2022). Pore-scale numerical simulations of flow and convective heat transfer in a porous woven metal mesh. *Chemical Engineering Science* 10, 150-159.
- Zhang Z. H., S. Mou and Z. G. Xu (2018). Experimental investigation on pool boiling mechanism of the gradient metal foam. In *International Heat Transfer Conference Digital Library*, Begel House Inc.
- Zhang, H., X. L. Wang and Y. Du (2021). Influence of heating surface size on heat transfer performance of saturated pool boiling. *Journal of Xi'an University of Science and Technology* 41(03), 417-424.
- Zhao, Z., J. Zhang and D. Jia (2017). Thermal performance analysis of pool boiling on an enhanced surface modified by the combination of microstructures and wetting properties. *Applied Thermal Engineering* 117, 417-426.
- Zhou, J., P. Z. Xu and B. J. Qi (2022). Effects of micro-pin-fins on the bubble growth and movement of nucleate pool boiling on vertical surfaces. *International Journal of Thermal Sciences* 171, 107186.
- Zhou, L. P., W. Li and T. X. Ma (2018). Experimental study on boiling heat transfer of a self-rewetting fluid on copper foams with pore-density gradient structures. *International Journal of Heat and Mass Transfer* 124, 210-219.
- Zhu, Y., H. T. Hu and G. L. Ding (2010). Influence of oil on nucleate pool boiling heat transfer of refrigerant on metal foam covers. *International Journal of Refrigeration* 34(2), 509-517.